

AN EXPLORATION OF HUMAN γ D-CRYSTALLIN AFFINITY FOR POTENTIAL AGGREGATION INHIBITORS: A MOLECULAR DOCKING INVESTIGATION

Călin G. FLOARE^{a*} , Adrian PÎRNĂU^a , Mihaela MIC^a ,
Elena MATEI^{a*} 

ABSTRACT. Cataract, the leading cause of blindness worldwide, is characterized by the presence of a cloudy area in the eye lens resulting in a loss of transparency. A number of mechanisms contribute to the longevity and transparency of the human lens, a reducing and oxygen deficient environment, the presence of UV-filters, and most importantly a unique supramolecular organization of its structural proteins, the α -, β - and γ -crystallins. With advancing age, progressively, or due to some mutations, this fragile equilibrium can be perturbed, causing γ -crystallin insolubilization, misfolding, fragmentation and aggregation.

In this study, we performed a comparative molecular docking analysis of several experimentally investigated molecules of natural origin, that might protect γ -crystallins from destabilization and aggregation. Our specific protein targets are wild-type human γ D-crystallin, and its mutant P23T γ D-crystallin, associated with congenital cataract. Thirteen phytochemicals were investigated as potential inhibitors of γ D-crystallin aggregation, and we compared their binding energies with those of lanosterol, an ingredient present in over-the-counter eye products, to prevent cataracts. We performed a detailed comparative molecular docking analysis and we found that the binding energies of lanosterol outcompete those of all the other investigated potential natural inhibitors.

Keywords: γ -crystallins, aggregation inhibitors, molecular docking

^a National Institute for Research and Development of Isotopic and Molecular Technologies, 67-103 Donat Street, 400293 Cluj-Napoca, Romania.

* Corresponding authors: calin.floare@itim-cj.ro, elena.matei@itim-cj.ro



INTRODUCTION

Crystallins, the predominant structural proteins in the eye lens, are the major contributors to the optimal refractive index necessary to focus light correctly into the retina. They must remain stable and soluble at very high concentrations throughout the entire life of the organism, to avoid the formation of light scattering aggregates [1, 2]. There are three major classes of crystallins in mammals, α -, β - and γ -crystallins. α -Crystallins (αA and αB) are members of the small heat-shock proteins superfamily [3-5] and are found in many cells and organs outside the lens. For instance, αB -crystallin was found to be expressed in the retina, heart, skeletal muscles, skin, brain and other tissues and to be overexpressed in several neurological disorders and in other cells known to be involved in many diseases, or in stressed cell lines. The small heat-shock α -crystallins suppress thermally induced aggregation of various enzymes and proteins, including that of β - and γ -crystallins, and represent ~40% of the eye lens proteins [6]. They are larger and polydisperse, multimeric proteins, that tend to form high molecular weight oligomers with sizes between 0.5 and 1MDa [7]. The β - and γ -crystallins are evolutionarily related and belong to the $\beta\gamma$ -crystallin superfamily, which also contains nonlens members in both prokaryotes and eukaryotes [8-10]. They contain aromatic and sulfur-rich residues with very compact intramolecular packing and have two homologous domains connected by a linker peptide [11]. β -Crystallins associate to form dimers up to octamers, and γ -crystallins, which range from 20-22 kDa, are monomers in solution [12]. γ -Crystallins are located in the central lens nucleus, and are one of the longest-lived proteins in the human body, without protein turnover, and can reach very high concentrations (~400 mg/ml in mammalian eye, and ~1000 mg/ml in some fish lenses).

Cataract affects a great majority of people and its incidence increases with age. It was estimated that more than 150 million people have impaired vision due to cataract [13]. Of these, more than 17 million people are blind, and approximately 28000 new cases are reported daily worldwide [14]. Even if good vision can be restored with an intraocular lens implant, posterior subcapsular opacification can occur in 10% of cases [15]. Therefore, identifying more robust and natural ways to prevent cataracts, is highly desirable.

The extraordinary transparency and longevity of the mammalian lens are due to the quasi-anoxic and reducing environment with antioxidant defenses and high glutathione levels [16], the presence of UV filters [17] and, most importantly, the particular composition and organization of its structural proteins, α -, β - and γ -crystallins. In the central part of the lens, the concentration of γ -crystallins can reach ~400 mg/ml [18], which over time or due to some congenital or external factors may locally increase and γ -crystallins aggregate.

AN EXPLORATION OF HUMAN γ D-CRYSTALLIN AFFINITY FOR POTENTIAL AGGREGATION INHIBITORS: A MOLECULAR DOCKING INVESTIGATION

Their delicate supramolecular equilibrium is maintained and the aggregation is additionally prevented by α -crystallins, which act as chaperones.

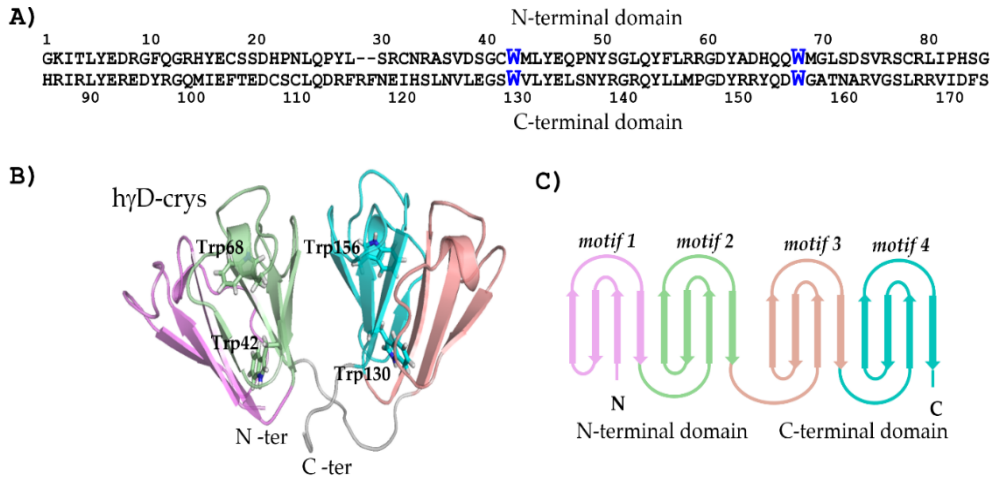


Figure 1. Human γ D-crystallin structure. A) Amino acid sequence of human γ D-crystallin, in the upper part N-terminal domain (N-ter) and in the lower part, C-terminal domain (C-ter). Tryptophan residues which contribute to the packing of the hydrophobic core and strongly quench the UV fluorescence are highlighted in blue. B) A ribbon representation of human γ D-crystallin. The four tryptophan residues are shown in stick representation. C) The complex topology of the γ D-crystallin domain constructed from four intercalated antiparallel β -sheet Greek key motifs, separated into two domains, joined by a short loop. Each motif is colored differently.

The human γ D-crystallin protein (h γ D-Crys), represented in Figure 1, is the third most abundant γ -crystallin in the lens and a significant component of the age-onset cataracts. It is a highly soluble monomeric protein composed of 173 amino acids arranged in two structurally homologous domains. Each domain is composed of two β -sheet Greek key motifs (see Figure 1C), a characteristic structural feature of the γ -crystallin family. The domains are connected by a linker peptide and form a highly conserved hydrophobic interface that plays a crucial role in determining long-term stability. In mammals, each domain of γ -crystallin contains a pair of conserved Trp residues, which contribute to the packing of the hydrophobic core and strongly quench UV fluorescence [19, 20]. The balance of interactions required to maintain short-range order between the constituent proteins of the eye lens is delicate, and it has been demonstrated that the γ D-crystallin protein can undergo irreversible

phase separation. In particular, the mutant protein P23T γ D-crystallin (h γ D-P23T) in which the amino acid proline at position 23 is replaced by a threonine, is associated with congenital cataracts [21]. Biochemical analyses of this mutant protein demonstrated that the solubility of h γ D-P23T, is dramatically lower than that of the wild-type h γ D-crystallin (h γ D-WT) protein, due to self-association into higher molecular weight amorphous aggregates under native conditions (neutral pH=7, 37°C) [13, 22-24]. These amorphous-looking deposits have a high degree of structural homogeneity at the atomic level retaining a native-like conformation, as revealed by solid-state NMR [21]. The Pro23 to Thr mutation has been associated with a number of known cataract phenotypes. Additionally, the h γ D-P23T mutant protein exhibit an inverse dependence of its solubility with temperature. The protein aggregates melt as the temperature of the solution decreases [24]. This particular behavior is similar to that we previously observed in a system containing cyclodextrins, methylated pyridines and some water, which presented a liquid-to-solid reentrant phase transition upon heating [25].

Structure-based docking screening is common in early drug discovery and molecular docking is a fast way to identify the prevailing binding modes of a ligand to a protein and of their particular interactions at the atomic level. Due to its facility of use, speed and cost-effective exploration of vast chemical space to identify a subset of potential hits for a target, it is currently routinely used by researchers to supplement the experimental studies. However, in too many cases, too harsh or inappropriate approximations are used, which results in undersampling of possible configurations which materializes into inaccurate predictions of the lowest binding energies. This reality prevents trustable comparisons between docking results obtained by different groups even if they are performed with practically the same software and complicates the situation even more if different software is used. The likelihood of obtaining valuable results from molecular docking simulations is directly related to the establishment of good practices and controls prior to undertaking a large-scale prospective screen. A good description of the major challenges is presented in a recent contribution [26]. The present research was initiated due to these identified limitations and our aim was to develop a detailed workflow and, ultimately, a database containing carefully performed simulations. This database contains detailed information about the crystallographic molecular structures of the proteins or macromolecules used and their structural pre-processing before the simulations, simulation parameters and the number of runs. We aim to standardize molecular docking simulations or at least to establish a good protocol in order to obtain reproducible and trustworthy results, in agreement with Aci-Sèche *et al.* [27]. In this article, we gathered and we present such a workflow, particularly exploring the molecular association between human

γ D-crystallin and a series of potential natural inhibitors of its aggregation, compared with that of lanosterol, an ingredient which is present in over-the-counter eye products used to prevent cataracts. In all our simulations performed to identify the most stable complexes between ligands and the h γ D-WT and h γ D-P23T crystallin proteins, we used AutoDock software. A comparative and trustworthy analysis, of the specific molecular interactions between γ D-crystallin proteins and small ligands can then provide valuable information, even at this level of theory, that contributes to the understanding and possibly to the control of the biochemical and biophysical interactions between these exceptional proteins constituting the eye lens. Consequently, in this study, we only present in detail the extended molecular docking analysis. Comprehensive *in vitro* aggregation suppression assays of h γ D-WT and h γ D-P23T are still underway and will be independently reported when completed.

RESULTS

Lanosterol

We initiated this study by thoroughly analyzing of the interaction between lanosterol and h γ D-WT and h γ D-P23T mutant. The tetracyclic triterpenoid lanosterol, from which animal and fungal steroids are derived, has been identified as an important component for maintaining the clarity of the eye lens [28]. Additionally, during a preclinical study lanosterol was identified as a possible agent for cataract remediation and prevention. Lanosterol, an amphipathic molecule present in the ocular lens, is synthesized by lanosterol synthase in a cyclization reaction of the cholesterol synthesis pathway. *In vivo* experiments in dogs have shown significant improvement in cataracts within 6 weeks of lanosterol injection [29]. In 2018, lanosterol was shown to improve lens clarity in cells with lens opacities due to aging or physical stressors [30]. A later study found positive results against lens opacification in cataract mice [31]. Lanosterol is currently used as an ingredient in over-the-counter eye products to prevent cataracts. However, because the solubility and bioavailability of lanosterol do not favor aqueous formulations, some researchers doubt its effectiveness [32]. Nevertheless, Heliostatix Biotechnology claims to have a method of solubilizing lanosterol for use in aqueous products and they already sell LumenPro, a vision eye care drop for animals with cataracts, that combines lanosterol and N-acetylcarnosine [33]. We consequently considered lanosterol, at this early stage of our analysis, as a point of reference. As we will see throughout the paper, this initial study was then followed by a comparative investigation of another 13 natural compounds with the potential

to counteract γ -crystallins misfolding and aggregation. This comparative theoretical analysis practically constitutes the subject of the actual paper. We performed this study as a necessary step before a thorough investigation of a more exhaustive search of potential inhibitors spanning the ZINC database [34, 35]. As mentioned above, our aim was to more closely evaluate the performance/precision for compound screening and to establish controls and a detailed workflow to further determine the reliability of the results.

In this study we performed an *in silico* ligand-protein molecular docking analysis which is currently a key tool in structural molecular biology and computer-assisted drug design. The goal is to predict the most likely binding mode(s) of a ligand to a protein with a known three-dimensional structure.

Prior to the actual docking calculations, we performed *first-principles* optimizations of the three-dimensional molecular structure of the ligands, to ensure that the three-dimensional molecular structure and the relative position of all atoms of the ligand were appropriate and correct from a chemical point of view. During the actual docking procedure, only the torsional angles of the bonds within the ligand are modified, following a Monte Carlo algorithm. Then, the molecule is docked to the protein, and this conformation is optimized through an energy minimization. The distances between the atoms of the ligand remain practically the same as those in the initial optimized conformation. As we also specified previously, the three-dimensional molecular structure of lanosterol was optimized using Gaussian 16 software [36] with the meta-GGA M06-2X hybrid functional and the 6-311++G(d,p) basis set. The same molecular conformation optimization was performed for all the molecules investigated in this study. As a result of the calculations, no imaginary vibrational frequencies were obtained, which proves that the optimized structure corresponds to a minimum of the potential energy surface (PES) and is not a transition state.

The chemical structure of lanosterol and the three-dimensional optimized conformation are shown in Figure 2. This was the molecular structure of the ligand used, on the following, by the docking algorithm.

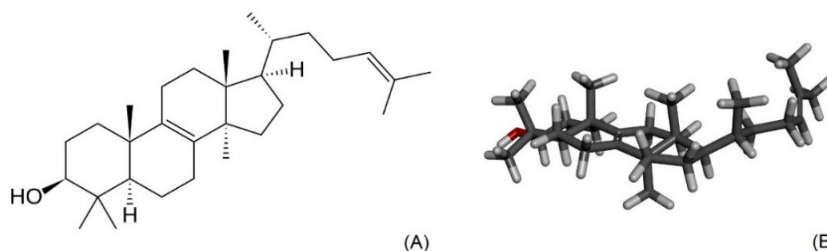


Figure 2. Lanosterol structure. (A) Lanosterol, $C_{30}H_{50}O$, molecular weight 426.7 g/mol (B) Molecular optimized structure of lanosterol using Gaussian 16 software with the meta-GGA M06-2X hybrid functional and the 6-311++G(d,p) basis set.

The conformations of the proteins were obtained from the structures deposited in the RCSB database, from the crystallographic one for h γ D-WT (PDB ID: 1HK0 [37]), and from the NMR determined solution structure for the h γ D-P23T mutant (2KFB [38]). To adapt them to the molecular docking process all the water molecules were removed. The docking procedure input files were generated using AutodockTools v. 1.5.6 [39, 40], the flexibility of the ligand was taken into account considering five torsion angles around the single bonds that were automatically detected in AutoDock, while the h γ D-crystallin conformations were kept rigid. AutoGrid software was used to generate interaction energy maps of the different types of atoms before actually performing the docking procedure. The maximum grid size was set to 126x126x126 points with a grid point spacing of 0.475 Å and the h γ D-crystallin conformations were fully included in the protein-centered cubic search volume. With the aim of obtaining good statistics and clustering distributions, as mentioned previously, we performed the highest number of runs accessible in AutoDock, 2000.

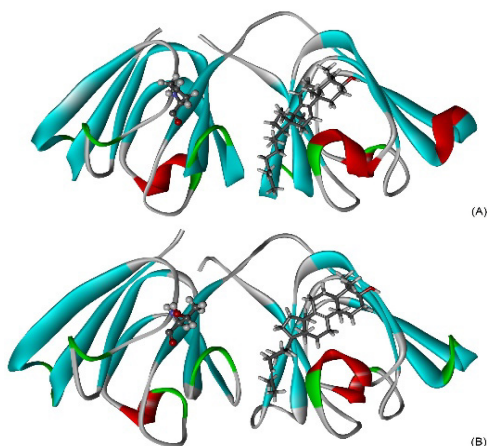


Figure 3. The lowest binding energies molecular docking conformations of lanosterol to (A) wild-type h γ D-WT and (B) the h γ D-P23T mutant. We also highlighted the amino acids at position 23 of polypeptidic chain.

Figure 3 shows the conformations with the lowest binding energies for the complex formed by lanosterol, and h γ D-WT and the h γ D-P23T variant, respectively.

The binding energies of these conformations are: -9.16 kcal/mol for the complex with h γ D-WT and -8.94 kcal/mol for the complex with h γ D-P23T. From the results obtained in the calculations, the binding of lanosterol to the h γ D-P23T mutant is less favorable, by approximately 0.22 kcal/mol, than that obtained for h γ D-WT. To better understand this difference, we mention that

after performing the 2000 runs, the obtained conformations were classified into families of similar conformations, denoted as “clusters” in Autodock and on the following. In Figure 4 we plot the histograms of the binding energy distributions of all the clusters identified during the analysis of docked conformations.

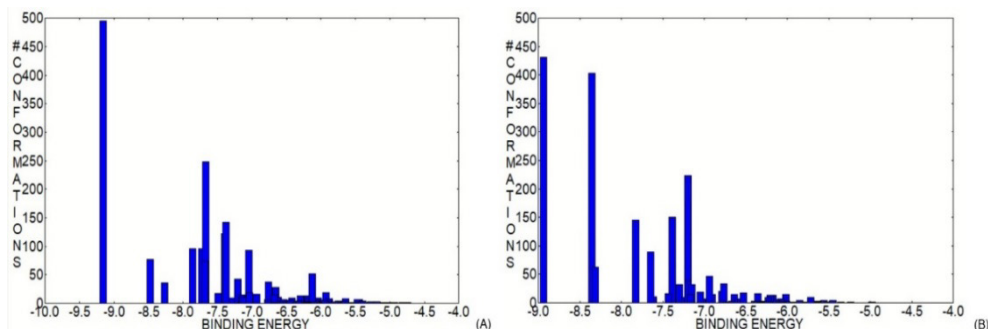


Figure 4. Histograms of the clusters of binding energies of lanosterol to hγD-crystallin: (A) hγD-WT and (B) the hγD-P23T mutant.

To properly grasp the meaning of these representations, we specify that the position of each cluster on the binding energy axis is determined only by the member with the lowest value of the binding energy of the cluster. In addition to the binding energy, another significant information is the frequency with which each binding conformation is identified, represented as the intensity in the histograms. As the number of members in a group/cluster increases, that particular binding conformation is more favored or has been identified more often. Other useful information, which can provide additional insight, is the range of binding energies of the members of each group, or at least the average binding energy of the group. With these specifications in mind, if we now analyze the results represented in Figure 4 we observe that the conformations with the lowest values of the binding energies also have the highest number of members in both cases, 495 for hγD-WT vs 431 in the case of the hγD-P23T mutant; the binding energy range of the members of these clusters is 3.45 vs 2.96 kcal/mol and the average binding energy is -8.0 vs -8.02 kcal/mol. This analysis demonstrated that these binding configurations were predominant and, as we can see, differed only slightly for the two proteins. In our opinion, these results prove that the method is reliable and stable, but still within a margin of error.

In Figures 5 and 6, we present a detailed analysis of the intermolecular interactions from the binding sites.

AN EXPLORATION OF HUMAN γ D-CRYSTALLIN AFFINITY FOR POTENTIAL AGGREGATION INHIBITORS: A MOLECULAR DOCKING INVESTIGATION

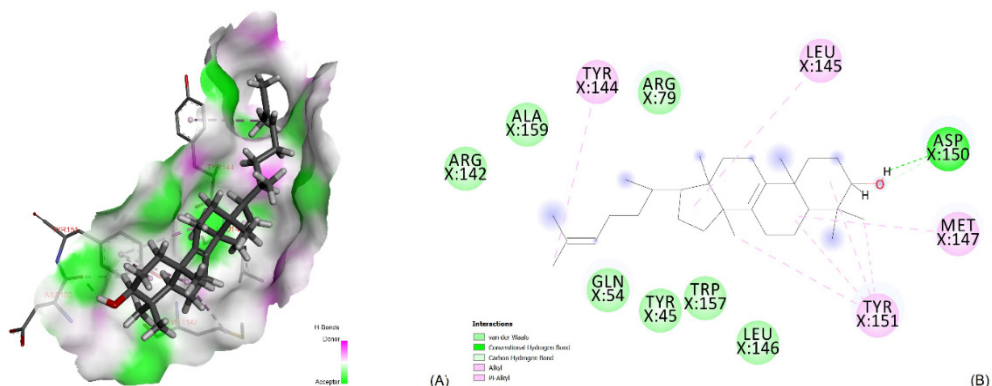


Figure 5. Proximity interactions within the binding site (A) and corresponding two-dimensional maps (B) between lanosterol and h γ D-WT.

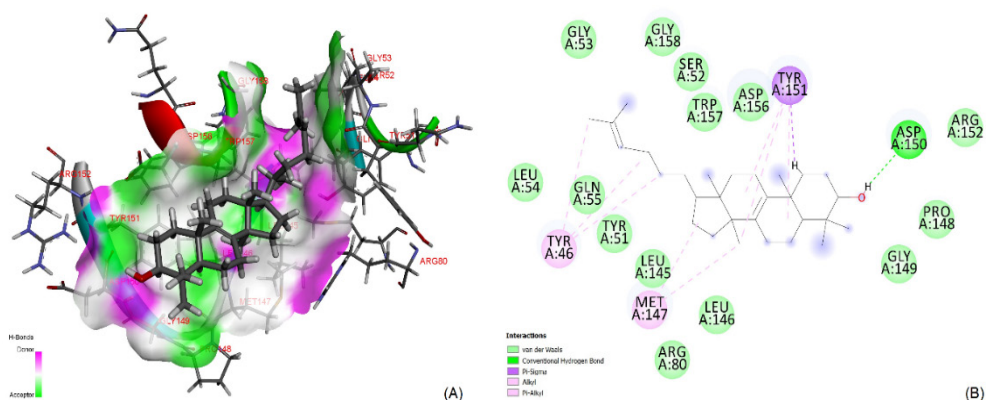


Figure 6. Proximity interactions within the binding site (A) and the corresponding two-dimensional maps (B) between lanosterol and the h γ D-P23T mutant.

As shown in Figure 3, the two conformations are quite similar, and the hydroxyl group of the lanosterol molecule interacts in both cases with the amino acids Asp150 and Tyr151 which are nearby. The lanosterol molecule seems to be only slightly displaced. During our analysis we noted that, in the PDB file containing the wild-type crystallographic h γ D-WT structure with RCSB ID: 1HK0, seems to be a numbering problem. Effectively, the amino acid number 86 does not exist, and we only have Gly85 and Ser87; however, in the 2KFB file, we have one additional glutamine residue from the His-tag tail at the N-terminus. In the file containing the h γ D-WT structure, the amino

acid glutamine does not appear, and the amino acid sequence starts normally with glycine (Gly1). We specify these inconsistencies because, in Figures 5 and 6, the amino acid numbering of the two proteins differs below position 85, due to these specific differences, after which the amino acid numbering becomes identical. We conclude this initial analysis by observing that molecular docking simulations successfully revealed the fact that lanosterol binds to a hydrophobic interfacial region near residues 135–165 on the C-terminal domain, a region that is crucial for hγD-Crys domain-swapping dimerization. This finding indicates that lanosterol binding likely disrupts the hγD-Crys dimerization and was also previously put in evidence by molecular dynamics simulations [41]. With all these theoretical predictions success, the binding of lanosterol to the C-terminal should, in practice, outcompete self-aggregation to be effective, and because lanosterol is poorly soluble in water, its effectiveness is uncertain [32]. The race for a better inhibitor is still on.

Potential natural inhibitors of hγD-crystallin aggregation

Finding an effective inhibitor to prevent or hopefully reverse of cataracts is a difficult endeavor. However, researchers do not give up hope and many theoretical and experimental studies have been conducted. There is an urgent need for inexpensive, nonsurgical approaches for the treatment of cataract for the reasons we extensively mentioned in the Introduction. High throughput theoretical [42] and experimental [6] studies have even been attempted. Given that considerable attention has been devoted to the search for phytochemical therapeutics, in this research we decided to focus on and comparatively investigate mainly flavonoids. This decision to investigate this class of polyphenols is based on the observation that several pharmacological actions of flavonoids may operate in the prevention of both age-related and diabetic cataracts. Flavonoids can affect multiple mechanisms or etiological factors responsible for the development of sight threatening ocular diseases including oxidative stress, nonenzymatic glycation and the polyol pathway and numerous studies have been conducted [43-52]. The interest in the other phytochemicals included in our study has been raised because a potential anti-cataract activity has been previously identified or studied: chlorogenic acid [53], curcumin [54-60], resveratrol [61-63], vitedoin A [43, 64], and ellagic acid [65, 66]. As shown in Table 1 and Figure 7, we list and graphically represent all 2D chemical structures of the investigated natural potential γ-crystallin aggregation inhibitors in this work.

AN EXPLORATION OF HUMAN γ D-CRYSTALLIN AFFINITY FOR POTENTIAL AGGREGATION INHIBITORS: A MOLECULAR DOCKING INVESTIGATION

Table 1. Investigated natural compounds with the potential to protect γ -crystallins from misfolding and aggregation.

Natural compounds	Plant	ZINC code
Apigenin	<i>Origanum vulgare</i>	ZINC000003871576
Luteolin	<i>Olea europaea</i>	ZINC000018185774
Eriodictyol	<i>Thymus vulgaris</i>	ZINC000000058117
Quercetin	<i>Allium cepa</i>	ZINC000003869685
Myricetin	<i>Spinacia oleracea</i>	ZINC000003874317
Genistein	<i>Fabaceae (Glycine max)</i>	ZINC000018825330
Vitexin	<i>Crataegus pinnatifida</i>	ZINC000004245684
Isovitexin	<i>Crataegus pinnatifida</i>	ZINC000004095704
Chlorogenic acid	<i>Vaccinium angustifolium</i>	ZINC000006482465
Curcumin	<i>Curcuma longa</i>	ZINC000100067274
Resveratrol	<i>Vitis vinifera</i>	ZINC000000006787
Vitedoin A	<i>Vitex negundo</i>	ZINC000014883365
Ellagic acid	<i>Rubus fruticosus</i>	ZINC000003872446

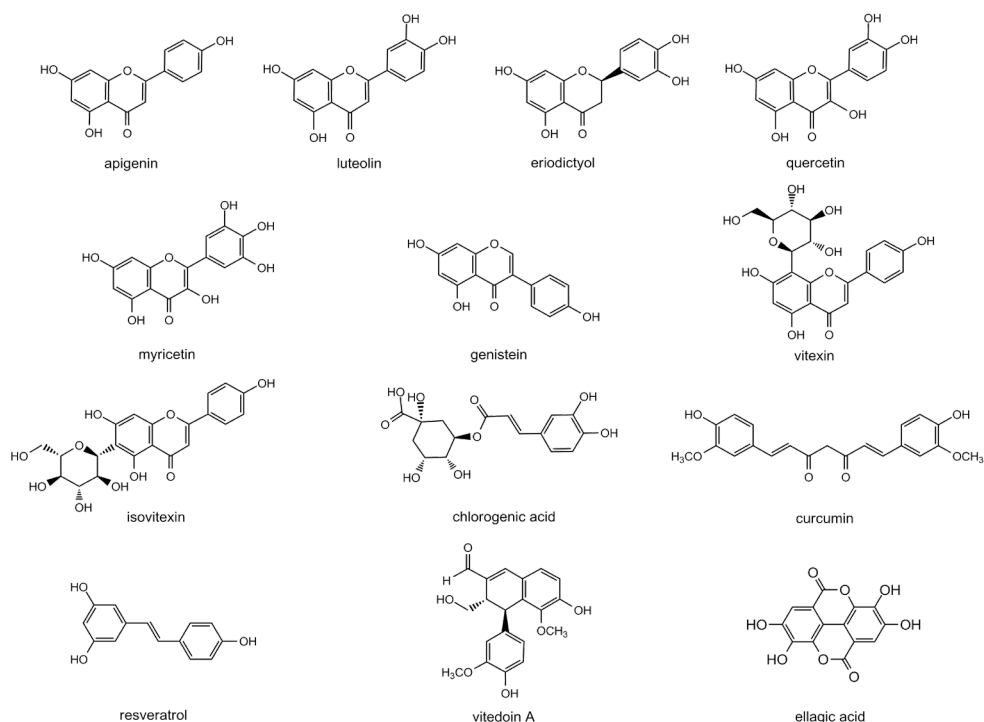


Figure 7. Chemical structures of natural compounds analyzed as potential cataract inhibitors.

We present the results obtained after performing docking calculations identical to those for lanosterol for all potential natural inhibitors specified and represented in Figure 7. All of them were docked on the same h_yD-WT and h_yD-P23T proteins with RCSB IDs: 1HK0 and 2KFB, respectively, using the same calculation parameters. Our aim was not only to theoretically identify a potential natural inhibitor of h_yD-crystallin aggregation with improved properties compared with lanosterol but also, as mentioned, to test the reliability of the molecular docking procedure for this particular case.

In Table 2 we present the results obtained for the leading conformations of all the potential natural inhibitors investigated in interaction with both, h_yD-WT and h_yD-P23T proteins. We specify for each one, the binding energy of the best docked conformation, the mean binding energy of the members in its cluster and also the number of the members of the cluster to which this conformation belongs. As shown in the table, for genistein, resveratrol and curcumin, we specified two entries. When both genistein and resveratrol were docked to the h_yD-P23T mutant protein we identified two lowest binding energy conformations. We mention them because, for genistein, both structures had the exact lowest binding energy but are docked to two different binding sites.

Table 2. Binding energies of the best docked conformations of investigated natural compounds to the h_yD-WT (RCSB ID: 1HK0) and the h_yD-P23T mutant (RCSB ID: 2KFB).

Compound	Lowest	Mean	Number	Lowest	Mean	Number
	Binding Energy	Binding Energy	in Cluster	Binding Energy	Binding Energy	in Cluster
	wild-type h _y D-WT - 1HK0			mutant h _y D-P23T - 2KFB		
Apigenin	-8.15	-7.20	275	-6.27	-5.99	214
Luteolin	-8.23	-7.17	157	-6.50	-5.88	395
Eriodictyol	-7.53	-6.48	53	-6.68	-6.35	786
Quercetin	-8.32	-7.15	192	-6.37	-5.71	403
Myricetin	-8.34	-6.92	118	-6.24	-5.56	355
Genistein	-8.90	-8.02	314	-6.19	-5.83	36
				-6.19	-5.79	194
Vitexin	-7.22	-6.22	92	-6.18	-4.77	206
Isovitexin	-7.08	-5.50	52	-6.50	-5.58	1452
Chlorogenic Acid	-6.81	-5.14	18	-6.13	-4.68	76
Curcumin enol-keto	-7.69	-6.67	7	-7.36	-5.94	210
Curcumin diketo	-8.95	-6.33	11	-7.16	-5.88	217
Resveratrol	-7.80	-6.98	77	-5.97	-5.47	165
				-5.93	-5.44	472
Vitedoin A	-6.71	-5.85	16	-6.16	-5.01	240
Ellagic Acid	-7.89	-7.31	477	-7.66	-7.30	109

For resveratrol, we again specified two most probable docking conformations, because the difference in energy between them was small enough. For curcumin we performed the calculation for both known curcumin tautomers: enol-keto and diketo. We considered both conformations relevant to be specified also to underline and point out the uncertainties of the molecular docking method on which we will further elaborate in the following.

By analyzing the results presented in this table, we observed that the values of the binding energies with the h γ D-WT protein are generally lower than with the h γ D-P23T mutant. For all the molecules investigated, we computed a mean of approximately -7.8 kcal/mol versus -6.5 kcal/mol, suggesting a stronger binding of all investigated compounds with h γ D-WT. This finding is opposite to what we initially expected to provide evidence and we observed this behavior during the initial calculation of lanosterol docking, as well. We specify here that we have not yet measured, experimentally, how a particular inhibitor interacts comparatively with the h γ D-WT protein versus the h γ D-P23T mutant and we did not find or know of a previous study to use it as a comparison. However, we know that the h γ D-P23T mutant aggregates at significantly lower concentrations than does h γ D-WT [21, 67]. This is what effectively motivated us to initiate this study to try also to understand how a single point mutation can have a drastic effect on the affinity and statistical equilibrium between these proteins and how this equilibrium can be influenced.

Even if a more precise investigation is necessary to clarify this theoretical result, we presume that the higher affinity obtained for all the molecules investigated for h γ D-WT could essentially be caused by the fact that the two protein structures were not determined under the same experimental conditions. The structure of h γ D-WT was solved by X-ray crystallography, while the structure of h γ D-P23T was solved using NMR in solution, and all atoms belonging to proteins were kept rigid during the calculations. We also emphasize here that we analyzed the affinity between several small potential inhibitors and h γ D-P23T as a monomer, without considering any details regarding the protein-protein interactions causing aggregation of this mutant. After this important preliminary observation, we will now continue our analysis since much relevant information is still hidden in the details of the best docking conformations. In the following, we will refer, to the lowest binding energies values specified in Table 2 and to the practical docking conformations that, for a better comparison, are all represented in Figure 8. With the exception of vitexin, all flavonoids here prefer docking in the same pocket created between the C-terminal tail and the linker between the N- and C- terminal domains, when interacting with h γ D-WT. Additionally, with the exception of genistein and vitexin, all the flavonoids preferentially dock in the same pocket belonging to C-terminal domain, when interacting with h γ D-P23T mutant protein. This comparative result suggested that protein pockets can accommodate molecules of various dimensions, with different affinities. If, between flavonoids, for the

hyD-WT, genistein leads with a binding energy of -8.9 kcal/mol, to the hyD-P23T mutant protein it is eriodictyol which has the lowest binding energy of -6.68 kcal/mol, and genistein does not have a high affinity for the mutant protein. We remark here also that the binding energies differ only by a maximum of 0.5 kcal/mol, vitexin having a binding energy of -6.18 kcal/mol.

When we compared the binding energies of all investigated molecules to the hyD-P23T mutant we observed that resveratrol, as a result of our calculations, was the least bound molecule. For resveratrol, we chose to present here two configurations bound to the hyD-P23T mutant with very close binding energies of -5.97 kcal/mol and of -5.93 kcal/mol. We represent this additional structure, because it was identified with preference (its cluster has 492 members versus 165 for the leading conformation) and because, as we can see in Figure 8, it binds in the same pocket belonging to C-terminal domain which extends in the space between N- and C- terminal domains, as the majority of flavonoids.

In Figure S17 from the Supplementary Material, we additionally present the histograms of the clusters of binding energies for all investigated potential natural inhibitors. In practical analysis, histograms are of crucial importance. Besides the fact that histograms aid in the identification of protein binding sites and of most stable configuration they also provide a practical, ordered and interactive view, inside AutoDockTools, of the identified clusters of conformations.

As an example, for genistein, if we look at the histogram representation for the interaction with hyD-P23T mutant protein, we observe that we obtained two clusters of conformations superposed at the lowest value of the binding energy, one with 36 members and another with 194. This is the reason why we both specified in Table 2 and Figure 8, as mentioned above, genistein (a), the leading conformation of the cluster having 36 members and genistein (b) the leading conformation of the cluster with 194 members. For resveratrol, as shown in Figure 8, the conformation named resveratrol (a) has the binding energy -5.97 kcal/mol and belongs to the cluster with 165 members only. After analyzing the favorite binding pockets for the hyD-WT and hyD-P23T mutant more generally, in Figure 8, we observe that those preferred by the majority of flavonoids are also “popular” for other molecules too, with some particular exceptions. We remarked here that vitexin, which is bulkier and has a greater lateral dimension and probably does not fit into the pocket created between the C-terminus and the linker between the N- and C- terminal domains, ultimately binds to the space between the N- and C- terminal domains. Isovitexin, on the other hand, respect the trend of preferred binding sites of the majority of flavonoids to both proteins even though it was slightly less stable than vitexin for the hyD-WT protein and more stable than vitexin when docked to the hyD-P23T mutant. Chlorogenic acid which binds in a somewhat reversed

AN EXPLORATION OF HUMAN γ D-CRYSTALLIN AFFINITY FOR POTENTIAL AGGREGATION INHIBITORS: A MOLECULAR DOCKING INVESTIGATION

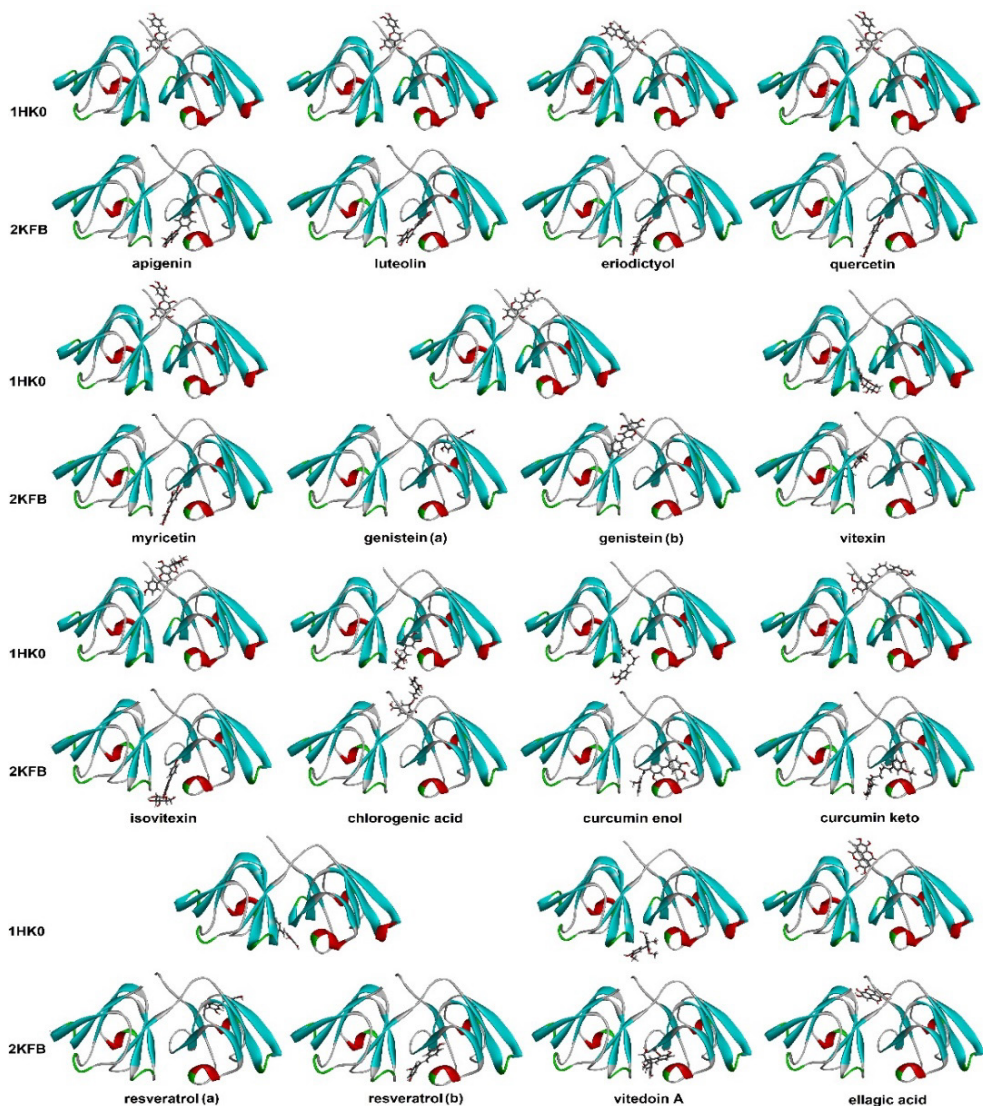


Figure 8. Lowest binding energies molecular docking conformations for all potential natural aggregation inhibitors to h γ D-WT (RCSB ID: 1HK0) and h γ D-P23T mutant (RCSB IDs: 2KFB) investigated in this work, ordered horizontally. To facilitate comparisons between these conformations, we represented them together. We kept the same order of the molecules investigated in this work, as previously specified in Figure 2. Proximity interactions within the binding site and their corresponding two-dimensional interaction maps are presented in Figures S1-S16 from the Supplementary Material.

manner to the abovementioned trend created by the majority of flavonoids, but has a relatively low binding energy to both proteins if we compare it with the other investigated molecules. Another surprising behavior is that of curcumin, for which we calculated the docking of both well-known tautomers enol-keto and diketo. We observe here that diketo tautomer, with a binding energy of -8.95 kcal/mol, is the leader of all natural compounds investigated, followed by genistein with an energy of -8.9 kcal/mol when docked to h_YD-WT. The diketo conformer of curcumin is also between the most bound molecules to the h_YD-P23T mutant, with a binding energy of -7.16 kcal/mol, which is slightly higher than that of curcumin-enol, -7.36 kcal/mol, and of ellagic acid, -7.66 kcal/mol. The binding of diketo curcumin tautomer follows also the abovementioned trend created by the majority of flavonoids, and the same mentioned pockets are preferentially chosen for both proteins. The bindings of Vitedoin A and ellagic acid, which are bulkier, are not consistent with the trend observed for the majority of flavonoids. Vitedoin A did not show a good binding ability because it is the least bound molecule to the h_YD-WT protein, and is close to the value obtained for resveratrol, when docked to the h_YD-P23T mutant. Conversely, ellagic acid is the leading molecule when docked to the h_YD-P23T mutant, for which the lowest value of the binding energy is -7.66 kcal/mol. If we now compare the binding energies of the leader molecules for both h_YD-WT and h_YD-P23T, -8.95 kcal/mol for curcumin diketo and that of ellagic acid, with the values obtained initially for lanosterol, -9.16 kcal/mol for the complex with h_YD-WT and -8.94 kcal/mol for the complex with the h_YD-P23T mutant, we observe that lanosterol is clearly the leader.

These binding energy values correspond to an estimated dissociation constant (K_d), which ranges from ~2.4 μ M to ~30 μ M for h_YD-P23T mutant, with exception of resveratrol with an estimated K_d of ~45 μ M. In the case of h_YD-WT protein the estimated dissociation constant ranges from ~0.3 μ M to ~12 μ M. These are reasonable K_d values, indicating potential binding inhibitors. However, the binding energies computed by molecular docking are only theoretical estimations of the possibility of complex formation, and a more accurate affinity constant can be determined experimentally by Isothermal titration calorimetry (ITC), or Nuclear Magnetic Resonance (NMR).

DISCUSSION

The results obtained in this study showed that the interaction of all potential inhibitors investigated and also that of lanosterol is more favorable with h_YD-WT than with the h_YD-P23T mutant. For instance, for lanosterol, the difference in binding energy to the wild-type and mutant protein is relatively small (approximately 0.22 kcal/mol); however, for genistein isoflavone, the difference

in binding energy is ~ 2.7 kcal/mol. For ellagic acid, the difference is again only 0.23 kcal/mol, and for all the other investigated molecules, the difference varies within these two values. We mentioned that this behavior can be caused by the fact that we used two different protein structures obtained independently by different groups, one crystallographically determined and the other in solution, and not being perfectly similar in sequence of aminoacids. Additionally, there are numerous cases in the literature in which mutants have reduced affinity for ligands compared to the wild-type protein. For instance, previous studies have shown that mutations in the Cyanovirin-N lectin completely abolish the carbohydrate binding site either on domain A, or domain B, rendering those mutants devoid of antiviral activity [68].

On the other hand, although molecular docking simulations are generally reliable and fast compared to other simulation methods, they use many approximations. Thus, the presence of a solvent, water or buffer solution, plays a fundamental role, but in traditional molecular docking simulations, water molecules are not taken into account and protein conformations are kept rigid. In reality, interactions with water molecules and hydrogen bond formation, or conversely, the presence of hydrophobic groups in the composition of the molecule, determine the functional, packed conformations of proteins, as well as the particular interactions with ligands and the value of the stability constants of their complexes in water. As a result of interactions with the solvent molecules, protein-ligand interactions adapt, and the amino acids in the interaction area can change their position to a certain extent. In fact, the conformation of the ligand adapts slightly as a result of interactions with the protein but also due to the presence of water molecules. It is therefore expected, following these approximations, that the results have a certain margin of error. In our study we did not intend to neglect the advances in molecular docking simulations where the receptor flexibility [69] and the explicit hydration can be taken into account by modifying the force field to model explicit water molecules [70] or through the use of physics-based endpoint approximation methods, such as the Molecular Mechanics Poisson-Boltzmann Surface Area (MM-PBSA) and Molecular Mechanics Generalized Born Surface Area (MM-GBSA). The main reason for our classic approach is that even if the accuracies of these advanced methods are usually higher than those of empirical scoring methods, the correlation between estimated and experimental binding free energies varies from system to system [71]. This is probably because the presence of other similar proteins in the immediate vicinity also plays an essential role in the more accurate description of the interactions involved. Temperature and pH are also critical parameters that influence interactions. Molecular dynamics simulations explicitly consider the presence of solvent molecules and can consider multiple proteins in the system but involve an incomparably greater computational effort [72].

Despite these, our calculations showed that lanosterol preferentially binds to a potential dimerization interface in the C-terminal domain of h γ D-Crys, which may provide protection from aggregation and cataract formation and this was also shown via molecular dynamics and free energy profile (FEP) calculations [41]. The fact that its binding energy is higher than that of all other investigated potential natural inhibitors must not be considered as a drawback also, but rather attributed to the particular structure of lanosterol and its specific binding mode. The out-of-plane methyl groups provide the molecule with an enlarged hydrophobic surface, leading to an enhanced binding affinity at the hydrophobic interface. Additionally, as the binding is mostly vdW-driven it seems that the hydrocarbon branches anchor to the hydrophobic site, reducing the mobility of the ligand and enhancing its binding stability.

Among the natural inhibitors studied, genistein, curcumin and ellagic acid had the lowest binding energies to h γ D-crys. We are actually extending these calculations to other potential inhibitors, and we plan experimental tests.

The comparative investigation presented in this article revealed that the *in silico* screening of inhibitors against the aggregation of h γ D-crystallin is not a simple task and requires considerable time and quite significant computing power. The system whose behavior we analyze at the molecular level is complex. Since only the analysis of a single inhibitor requires considerable time on the order of an entire day on a single workstation for a well performed molecular docking simulation or several days to calculate a long enough molecular dynamics trajectory on a high-performance parallel computer, it is somehow illusory to aim for an exhaustive analysis of hundreds, thousands or millions of compounds available in the ZINC organic molecular compound database. High-throughput screening of the ZINC database on moderately sized computer clusters requires not much more than 1 s/molecule/core (1 ms/configuration) [26] but this can result in undersampling of possible configurations. Even if large scale docking can be attempted with the recently developed AutoDock-GPU [73], targeting a subset of the ZINC database is a more feasible approach. This was our initial motivation when we chose to analyze, as carefully possible at this level of the theory, the docking of flavonoids in this study. A substantial effort must be consequently dedicated to the most rational and documented determination of this subset based on the knowledge of the possible interactions involved, as well as the identification and analysis of the interaction surface between the h γ D-P23T mutant aggregating protein ensemble. A more promising strategy could be to infer the structure of a potential inhibitor by analyzing the interaction domains between the monomers and understanding how the Pro23Thr mutation favors this interaction. This can be investigated within relatively short nonequilibrium molecular dynamics simulations and the simulations can also be performed at various temperatures. From a personal experience during molecular dynamics studies of the liquid-solid reentrant

phase transition upon heating in methylated pyridines containing cyclodextrins, temperature plays an important role in the stability of the system [25]. Similar simulations were recently performed and reported by Brudar and Hribar-Lee [74] and Zhou *et al.* [41, 75].

The identification of a non-surgical cataract remedy remains a real challenge to which we are committed and new contributions from our group will follow.

CONCLUSIONS

In this study, the affinities of h γ D-crystallin, the wild-type and the P23T mutant were explored using the lanosterol molecule as a reference. We performed molecular docking calculations for 13 phytochemicals identified as molecules potentially inhibiting h γ D-crystallin aggregation that were previously studied experimentally and reported in the literature, and we compared their binding energies with that of lanosterol. Initially, we observed that all the investigated molecules had a greater affinity for h γ D-WT than for the h γ D-P23T mutant. Even if this result must be checked using more precise methods for binding energy estimation or experimentally, we most likely associated this result with the particular h γ D-crystallin molecular structures determined, one by X-ray crystallography and the other using liquid NMR, which were kept rigid during our calculations. The second observation was that the binding energies of the lanosterol, which was used as a reference, outcompeted those of all the other investigated potential natural inhibitors. This result, however, must not be taken as a drawback of this study but rather attributed to the particular structure of lanosterol and to its specific binding mode to a hydrophobic interfacial region near the C-terminal domain, a region crucial for h γ D-Crys domain-swapping dimerization. This binding mode is similar to that previously identified by more accurate molecular dynamics simulations [41] and proves the reliability of molecular docking simulations as initial binding mode approximation. According to the comparative analysis of all 13 phytochemicals investigated, genistein, curcumin and ellagic acid had the lowest binding energies to h γ D-crystallins but still higher than that of lanosterol. Ongoing efforts are underway to improve and extend these calculations to other potential inhibitors following the new and innovative ideas.

COMPUTATIONAL DETAILS

Screening for inhibitors of h γ D-P23T mutant aggregation is a real challenge and requires considerable time and resources. The architecture of structural eye lens proteins is complex and, in this study, we explored drug

affinity of the human γ D-crystallin protein, which has been proven to be a significant component of the age-onset cataracts.

Because the analysis of hundreds or thousands of compounds needs the availability of a large computing cluster and an exhaustive analysis of millions compounds available in the ZINC database is practically impossible, in this first approach, we theoretically analyzed a relatively small subset of thirteen potential natural inhibitors we identified in the literature. Lanosterol was used as a reference. Prior to the actual docking calculations, the molecular structures of all potential γ D-crystallin aggregation inhibitors were optimized with Gaussian 16 software [36] using the meta-GGA M06-2X hybrid functional and the 6-311++G(d,p) basis set and no imaginary frequencies were obtained. The molecular conformations of γ D-WT and the γ D-P23T mutant were identified in the RCSB database (PDB ID: 1HK0 [37] and 2KFB [38]) and the three-dimensional molecular structures used in our calculations were extracted from these conformations. Computational molecular docking with the aim of obtaining the most feasible interaction conformations between the chosen potential aggregation inhibitors and γ D-crystallin was then performed using the Monte Carlo simulated annealing search implemented in AutoDock v4.2 [39].

AutoDockTools v 1.5.6 [39, 40] was used to prepare the input docking files and pdbqt files, which include the atomic coordinates (PDB), partial charges (Q) and atom types (T) in one file. We initially added all the hydrogens to both molecules. Following the AutoDock standard docking procedure, all nonpolar hydrogen atoms and their charges were then automatically merged with their parent carbon atom. Atomic charges were calculated using the Gasteiger-Marsili method [76].

The flexibility of all natural potential inhibitors has been taken into account by setting up torsion angles around the rotatable bonds, automatically detected by the AutoDock ligand input procedure. All atoms of both γ D-crystallin proteins were kept rigid. Prior to the actual docking run, AutoGrid was used to precalculate grid maps of the interaction energies of various atom types. The grid size was set to $126 \times 126 \times 126$ points with 0.475 Å grid point spacing, and the cubic search box was centered on the γ D-crystallin protein and surrounding it.

The Lamarckian genetic algorithm [77, 78], which iteratively generates and optimizes a population of ligand conformations, was used to search for the best conformers, the global search space being mainly sampled. The default parameters, automatically set up by AutoDockTools, which are also mentioned in detail in our previous contributions [79-81], were used: the initial population of random individuals had a population size of 150 individuals, the maximum number of energy evaluations per run was 2,500,000, maximum

number of generations was 27,000, with a rate of gene mutation of 0.02, a crossover rate of 0.8 and the cluster tolerance was 2 Å. To obtain good statistics and clustering, 2000 runs were performed, each starting with a different random generation seed. Visualization and analysis of the docking results were performed using Biovia Discovery Studio Visualizer v20.1 and Chimera v1.14 [82].

ACKNOWLEDGMENTS

This work was supported by the Romanian Ministry of Research, Innovation and Digitization (MCID), CNCS/CCCDI-UEFISCDI, Grant number PN-III-P4-PCE-2021-0316 and by the MCID through the “Nucleu” Program within the National Plan for Research, Development and Innovation 2022–2027, Project PN 23 24 01 05, and through the Installations and Special Objectives of National Interest (IOSIN), IZOSTAB. The computing resources used were provided by the High-Performance Computing Data Center of INCDTIM, Cluj-Napoca.

The authors declare that they have no conflicts of interest.

Supplementary material: Supplementary file and molecular docking simulations were uploaded on the Zenodo website and are available at the link <https://zenodo.org/records/13691397> (DOI: 10.5281/zenodo.13691397)

REFERENCES

1. G.J. Wistow, J. Piatigorsky, *Annu. Rev. Biochem.*, **1988**, *57*, 479-504.
2. H. Bloemendal, W. de Jong, R. Jaenicke, N.H. Lubsen, C. Slingsby, A. Tardieu, *Progress in Biophysics and Molecular Biology*, **2004**, *86*(3), 407-485.
3. W.W. Dejong, J.A.M. Leunissen, C.E.M. Voorter, *Mol. Biol. Evol.*, **1993**, *10*(1), 103-126.
4. J. Horwitz, *Exp. Eye Res.*, **2009**, *88*(2), 190-194.
5. J. Horwitz, M.P. Bova, L.L. Ding, D.A. Haley, P.L. Stewart, *Eye*, **1999**, *13*, 403-408.
6. S. Islam, M.T. Do, B.S. Frank, G.L. Hom, S. Wheeler, H. Fujioka, B. Wang, G. Minocha, D.R. Sell, X. Fan, K.J. Lampi, V.M. Monnier, *J. Biol. Chem.*, **2022**, *298*(10), 102417.
7. S. Bassnett, Y.R. Shi, G.F.J.M. Vrensen, *Philos. Tans. Roy. Soc. B*, **2011**, *366*(1568), 1250-1264.
8. N.H. Lubsen, H.J.M. Aarts, J.G.G. Schoenmakers, *Prog. Biophys. Mol. Bio.*, **1988**, *51*(1), 47-76.

9. G. Wistow, *Molecular Biology and Evolution of Crystallins: Gene Recruitment and Multifunctional Proteins in the Eye Lens*, Springer, R.G. Landes Co., Austin, TX., **1995**.
10. M.E. Ray, G. Wistow, Y.A. Su, P.S. Meltzer, J.M. Trent, *Prog. Nat. Acad. Sci. USA*, **1997**, *94*(7), 3229-3234.
11. A. Laganowsky, J.L.P. Benesch, M. Landau, L.L. Ding, M.R. Sawaya, D. Cascio, Q.L. Huang, C.V. Robinson, J. Horwitz, D. Eisenberg, *Protein Sci.*, **2010**, *19*(5), 1031-1043.
12. C. Slingsby, G.J. Wistow, A.R. Clark, *Protein Sci.*, **2013**, *22*(4), 367-380.
13. J.I. Clark, J.M. Clark, *Int. Rev. Cytology*, **1999**, *192*, 171-187.
14. Z. Kyselova, M. Stefek, V. Bauer, *J. Diabetes Complicat.*, **2004**, *18*(2), 129-140.
15. J. Konopinska, M. Mlynarczyk, D.A. Dmuchowska, I. Obuchowska, *J. Clin. Med.*, **2021**, *10*(13), 2847.
16. X.J. Fan, V.M. Monnier, J. Whitson, *Exp. Eye Res.*, **2017**, *156*, 103-111.
17. A.M. Wood, R.J.W. Truscott, *Exp. Eye Res.*, **1993**, *56*(3), 317-325.
18. V.P.R. Vendra, I. Khan, S. Chandani, A. Muniyandi, D. Balasubramanian, *Biochim. Biophys. Acta - Gen. Subjects*, **2016**, *1860*(1), 333-343.
19. M.S. Kosinski-Collins, S.L. Flaugh, J. King, *Protein Sci*, **2004**, *13*(8), 2223-2235.
20. J. Chen, P.R. Callis, J. King, *Biochemistry*, **2009**, *48*(17), 3708-3716.
21. J.C. Boatz, M.J. Whitley, M. Li, A.M. Gronenborn, P.C.A. van der Wel, *Nature Commun.*, **2017**, *8*(1), 15137.
22. P. Evans, K. Wyatt, G.J. Wistow, O.A. Bateman, B.A. Wallace, C. Slingsby, *J. Mol. Biol.*, **2004**, *343*(2), 435-444.
23. A. Basak, O. Bateman, C. Slingsby, A. Pande, N. Asherie, O. Ogun, G.B. Benedek, J. Pande, *J. Mol. Biol.*, **2003**, *328*(5), 1137-1147.
24. A. Pande, O. Annunziata, N. Asherie, O. Ogun, G.B. Benedek, J. Pande, *Biochemistry*, **2005**, *44*(7), 2491-2500.
25. M. Plazanet, C. Floare, M.R. Johnson, R. Schweins, H.P. Trommsdorff, *J. Chem. Phys.*, **2004**, *121*(11), 5031-5034.
26. B.J. Bender, S. Gahbauer, A. Lutten, J.K. Lyu, C.M. Webb, R.M. Stein, E.A. Fink, T.E. Balius, J. Carlsson, J.J. Irwin, B.K. Shoichet, *Nat. Protoc.*, **2021**, *16*(10), 4799-4832.
27. S. Aci-Sèche, S. Bourg, P. Bonnet, J. Rebehmed, A.G. de Brevern, J. Diharce, *Data Brief*, **2023**, *49*, 109386.
28. M.W. Huff, D.E. Telford, *Trends in Pharmacological Sciences*, **2005**, *26*(7), 335-340.
29. L. Zhao, X.-J. Chen, J. Zhu, Y.-B. Xi, X. Yang, L.-D. Hu, H. Ouyang, S.H. Patel, X. Jin, D. Lin, F. Wu, K. Flagg, H. Cai, G. Li, G. Cao, Y. Lin, D. Chen, C. Wen, C. Chung, Y. Wang, A. Qiu, E. Yeh, W. Wang, X. Hu, S. Grob, R. Abagyan, Z. Su, H.C. Tjondro, X.-J. Zhao, H. Luo, R. Hou, J. Jefferson, P. Perry, W. Gao, I. Kozak, D. Granet, Y. Li, X. Sun, J. Wang, L. Zhang, Y. Liu, Y.-B. Yan, K. Zhang, *Nature*, **2015**, *523*(7562), 607-611.
30. X. Shen, M. Zhu, L. Kang, Y. Tu, L. Li, R. Zhang, B. Qin, M. Yang, H. Guan, *J. Ophthalmol.*, **2018**, *2018*, 1-9.

31. K. Wang, M. Hoshino, K. Uesugi, N. Yagi, B.K. Pierscionek, U.P. Andley, *Investigative Ophthalmol. & Visual Sci.*, **2022**, 63(5), 15.
32. D.M. Daszynski, P. Santhoshkumar, A.S. Phadte, K.K. Sharma, H.A. Zhong, M.F. Lou, P.F. Kador, *Sci. Rep.*, **2019**, 9(1).
33. *Heliostatix Biotechnology*, **2023**. <https://Heliostatix.org>. (accessed 1st November 2023 2023).
34. J. Irwin, *Abstr. of Papers of Am. Chem. Soc.*, **2017**, 253.
35. J.J. Irwin, K.G. Tang, J. Young, C. Dandarchuluun, B.R. Wong, M. Khurelbaatar, Y.S. Moroz, J. Mayfield, R.A. Sayle, *J. Chem. Inf. Model.*, **2020**, 60(12), 6065-6073.
36. M. J. Frisch, G. W. Trucks, H. B. Schlegel, G. E. Scuseria, M. A. Robb, J. R. Cheeseman, G. Scalmani, V. Barone, G. A. Petersson, H. Nakatsuji, X. Li, M. Caricato, A. V. Marenich, J. Bloino, B. G. Janesko, R. Gomperts, B. Mennucci, H. P. Hratchian, J. V. Ortiz, A. F. Izmaylov, J. L. Sonnenberg, D. Williams-Young, F. Ding, F. Lipparini, F. Egidi, J. Goings, B. Peng, A. Petrone, T. Henderson, D. Ranasinghe, V. G. Zakrzewski, J. Gao, N. Rega, G. Zheng, W. Liang, M. Hada, M. Ehara, K. Toyota, R. Fukuda, J. Hasegawa, M. Ishida, T. Nakajima, Y. Honda, O. Kitao, H. Nakai, T. Vreven, K. Throssell, J. J. A. Montgomery, J. E. Peralta, F. Ogliaro, M. J. Bearpark, J. J. Heyd, E. N. Brothers, K. N. Kudin, V. N. Staroverov, T. A. Keith, R. Kobayashi, J. Normand, K. Raghavachari, A. P. Rendell, J. C. Burant, S. S. Iyengar, J. Tomasi, M. Cossi, J. M. Millam, M. Klene, C. Adamo, R. Cammi, W. Ochterski, R. L. Martin, K. Morokuma, O. Farkas, J. B. Foresman, D.J. Fox, *Gaussian 16, Revision C.02*, Gaussian Inc., Wallingford CT: **2016**.
37. A. Basak, O. Bateman, C. Slingsby, A. Pande, N. Asherie, O. Ogun, G.B. Benedek, J. Pande, *J. Mol. Biol.*, **2003**, 328(5), 1137-1147.
38. J. Jung, I.-J.L. Byeon, Y. Wang, J. King, A.M. Gronenborn, *Biochemistry*, **2009**, 48(12), 2597-2609.
39. G.M. Morris, R. Huey, W. Lindstrom, M.F. Sanner, R.K. Belew, D.S. Goodsell, A.J. Olson, *J. Comput. Chem.*, **2009**, 30(16), 2785-2791.
40. O. Trott, A.J. Olson, *J. Comput. Chem.*, **2009**, 31(2), 455–461.
41. H.S. Kang, Z.X. Yang, R.H. Zhou, *J. Am. Chem. Soc.*, **2018**, 140(27), 8479-8486.
42. F. Olawale, O. Iwaloye, I.M. Folorunso, S. Shityakov, *J. Comput. Biophys. and Chem.*, **2022**, 22(01), 11-30.
43. D. Tewari, O. Samoila, D. Gocan, A. Mocan, C. Moldovan, H.P. Devkota, A.G. Atanasov, G. Zengin, J. Echeverria, D. Vodnar, B. Szabo, G. Crisan, *Front. in Pharmacology*, **2019**, 10.
44. I. Sher-Rosenthal, E. Bubis, Z. Goldberg, M. Samara, A. Elmann, Y. Rotenstreich, *Invest. Ophth. Vis. Sci.*, **2021**, 62(8).
45. A.K. Ghosh, R. Thapa, H.N. Hariani, M. Volyanyuk, S.D. Ogle, K.A. Orloff, S. Ankireddy, K.R. Lai, A. Ziniauskaite, E.B. Stubbs, G. Kalesnykas, J.J. Hakkarainen, K.A. Langert, S. Kaja, *Pharmaceutics*, **2021**, 13(9).
46. S. Davinelli, S. Ali, G. Scapagnini, C. Costagliola, *Front. Nutr.*, **2021**, 8.
47. H. Matsuda, T. Wang, H. Managi, M. Yoshikawa, *Bioorgan. Med. Chem.*, **2003**, 11(24), 5317-5323.

48. H. Matsuda, T. Morikawa, I. Toguchida, M. Yoshikawa, *Chem. Pharm. Bull.*, **2002**, 50(6), 788-795.
49. B.S. Patil, G.K. Jayaprakasha, K.N.C. Murthy, A. Vikram, *J. Agr. Food. Chem.*, **2009**, 57(18), 8142-8160.
50. S. Majumdar, R. Srirangam, *J. Pharm. Pharmacol.*, **2010**, 62(8), 951-965.
51. W. Kalt, A. Hanneken, P. Milbury, F. Tremblay, *J. Agr. Food Chem.*, **2010**, 58(7), 4001-4007.
52. M. Stefek, *Interdiscipl. Toxicol.*, **2011**, 4(2), 69-77.
53. J.K. Song, D.D. Guo, H.S. Bi, *Int. J. Mol. Med.*, **2018**, 41(2), 765-772.
54. B.P. Mohanty, T. Mitra, S. Ganguly, S. Das Sarkar, A. Mahanty, *Biol. Trace Elem. Res.*, **2021**, 199(9), 3354-3359.
55. J.I. Choi, J. Kim, S.Y. Choung, *Mol. Vis.*, **2019**, 25, 118-128.
56. J. Cao, T. Wang, M. Wang, *BMC Ophthalmol.*, **2018**, 18, 48.
57. X.F. Liu, J.L. Hao, T. Xie, N.J. Mukhtar, W. Zhang, T.H. Malik, C.W. Lu, D.D. Zhou, *Front. in Pharmacol.*, **2017**, 8, 66.
58. J.H. Liao, Y.S. Huang, Y.C. Lin, F.Y. Huang, S.H. Wu, T.H. Wu, *J. Agr. Food Chem.*, **2016**, 64(10), 2080-2086.
59. C.G. Wang, L. Xu, F. Cheng, H.Q. Wang, L.Y. Jia, *RSC Adv.*, **2015**, 5(38), 30197-30205.
60. C.N. Grama, P. Suryanarayana, M.A. Patil, G. Raghu, N. Balakrishna, M.N.V.R. Kumar, G.B. Reddy, *Plos One*, **2013**, 8(10), 78217.
61. J.W.R. Wu, C.Y. Kao, L.T.W. Lin, W.S. Wen, J.T. Lai, S.S.S. Wang, *Biochem. Eng. J.*, **2013**, 78, 189-197.
62. A. Dawn, V. Goswami, S. Sapra, S. Deep, *Langmuir*, **2023**, 39(3), 1330-1344.
63. H. Nagashima, N. Sasaki, S. Amano, S. Nakamura, M. Hayano, K. Tsubota, *Sci. Rep.*, **2021**, 11(1), 2174.
64. B. Neha, R. Jannavi, P. Sukumaran, *J. Pharm. Res. Int.*, **2021**, 33(29a), 17-32.
65. J. Jeevanandam, R. Madhumitha, N.T. Saraswathi, *J. Mol. Struct.*, **2021**, 1226, 129428.
66. M. Sakthivel, P. Geraldine, P.A. Thomas, *Graef Arch. Clin. Exp. Ophthalmol.*, **2011**, 249(8), 1201-1210.
67. M.L. Broide, C.R. Berland, J. Pande, O.O. Ogun, G.B. Benedek, *Proc. Natl. Acad. Sci. USA*, **1991**, 88(13), 5660-5664.
68. E. Matei, A. Zheng, W. Furey, J. Rose, C. Aiken, A.M. Gronenborn, *J. Biol. Chem.*, **2010**, 285(17), 13057-13065.
69. P.A. Ravindranath, S. Forli, D.S. Goodsell, A.J. Olson, M.F. Sanner, *Plos Comput. Biol.*, **2015**, 11(12), e1004586.
70. S. Forli, A.J. Olson, *J. Med. Chem.*, **2012**, 55(2), 623-638.
71. L. El Khoury, D. Santos-Martins, S. Sasmal, J. Eberhardt, G. Bianco, F.A. Ambrosio, L. Solis-Vasquez, A. Koch, S. Forli, D.L. Mobley, *J. Comput. Aid. Mol. Des.*, **2019**, 33(12), 1011-1020.
72. X.B. He, S.H. Liu, T.S. Lee, B.H. Ji, V.H. Man, D.M. York, J.M. Wang, *ACS Omega*, **2020**, 5(9), 4611-4619.
73. D. Santos-Martins, L. Solis-Vasquez, A.F. Tillack, M.F. Sanner, A. Koch, S. Forli, *J. Chem. Theor. Comput.*, **2021**, 17(2), 1060-1073.

AN EXPLORATION OF HUMAN γ D-CRYSTALLIN AFFINITY FOR POTENTIAL AGGREGATION
INHIBITORS: A MOLECULAR DOCKING INVESTIGATION

74. S. Brudar, B. Hribar-Lee, *J. Mol. Liq.*, **2023**, 386, 122461.
75. P. Das, J.A. King, R.H. Zhou, *Proc. Natl. Acad. Sci. USA*, **2011**, 108(26), 10514-10519.
76. J. Gasteiger, M. Marsili, *Tetrahedron*, **1980**, 36(22), 3219-3228.
77. G.M. Morris, D.S. Goodsell, R.S. Halliday, R. Huey, W.E. Hart, R.K. Belew, A.J. Olson, *J. Comput. Chem.*, **1998**, 19(14), 1639-1662.
78. J. Fuhrmann, A. Rurainski, H.P. Lenhof, D. Neumann, *J. Comput. Chem.*, **2010**, 31(9), 1911-1918.
79. C.G. Floare, M. Bogdan, M. Tomoaia-Cotisel, A. Mocanu, *J. Mol. Struct.*, **2022**, 1248, 131477.
80. M. Mic, A. Pîrnau, C.G. Floare, M. Bogdan, *Int. J. Biol. Macromol.*, **2020**, 147, 326-332.
81. M. Mic, A. Pîrnau, C.G. Floare, G. Marc, A.H. Franchini, O. Oniga, L. Vlase, M. Bogdan, *J. Mol. Struct.*, **2021**, 1244, 131278.
82. E.F. Pettersen, T.D. Goddard, C.C. Huang, G.S. Couch, D.M. Greenblatt, E.C. Meng, T.E. Ferrin, *J. Comput. Chem.*, **2004**, 25(13), 1605-1612.